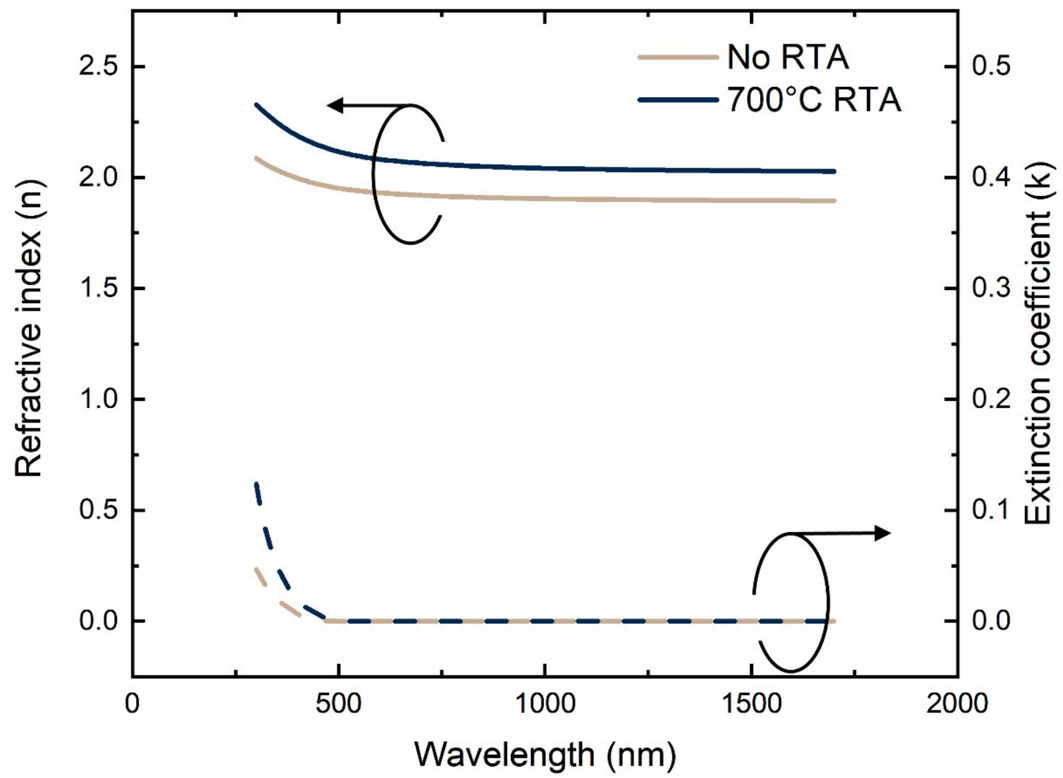

Fig. S1: Refractive index and extinction coefficient of PECVD SiN_x *before and after rapid thermal annealing (RTA).*

Fig. S1 shows the effect of rapid thermal annealing (RTA) on the optical properties of a 500 nm thick SiN_x film deposited on Si. A thickness of 500 nm is chosen for the bulk sample since thicker films experience stress-induced delamination. For the waveguides, such a stress-induced defect does not occur. The sample is annealed at 700°C under nitrogen atmosphere for 5-minute cycles of 10 s heating periods and 120 s cooling periods. Notably, the film thickness is kept at 500 nm, cracking during the annealing process.

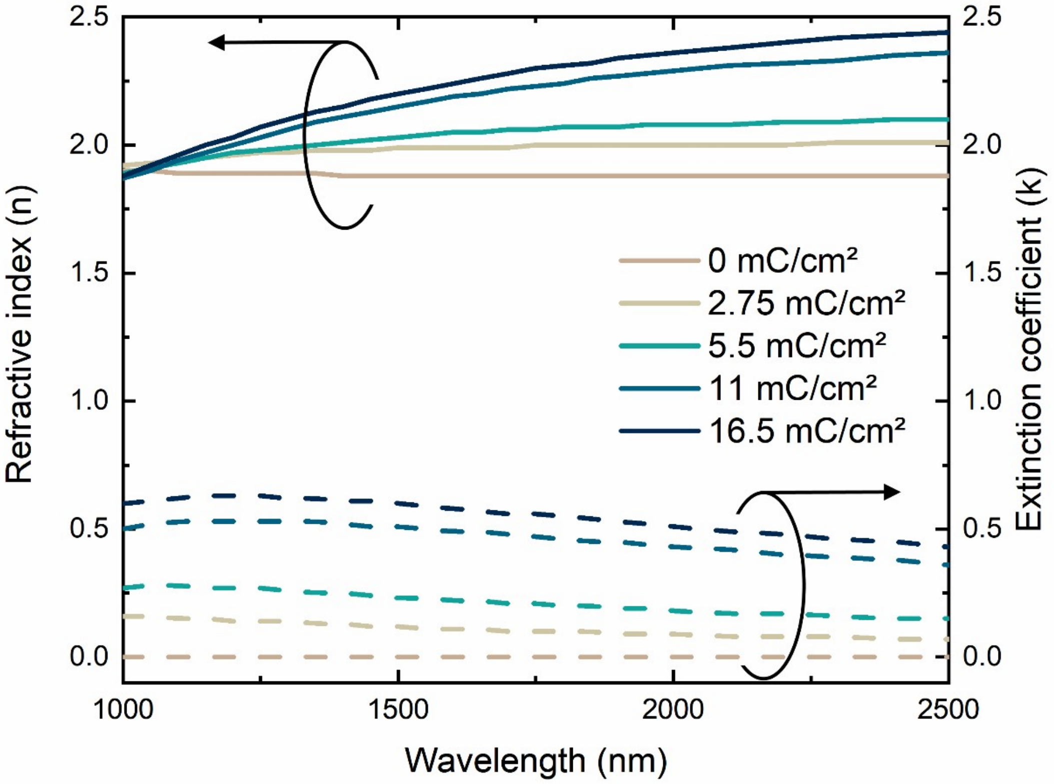

Fig. S2: Refractive index (n) and extinction coefficient (k) of WO_3 for different levels of Na^+ ion intercalation measured as charge per unit area.

Fig. S2 shows the refractive index, (n) and extinction coefficient (k) for WO_3 as a function of oxidation state. Na^+ ions are injected through a constant current from a 0.1 M $NaClO_4$ solution.

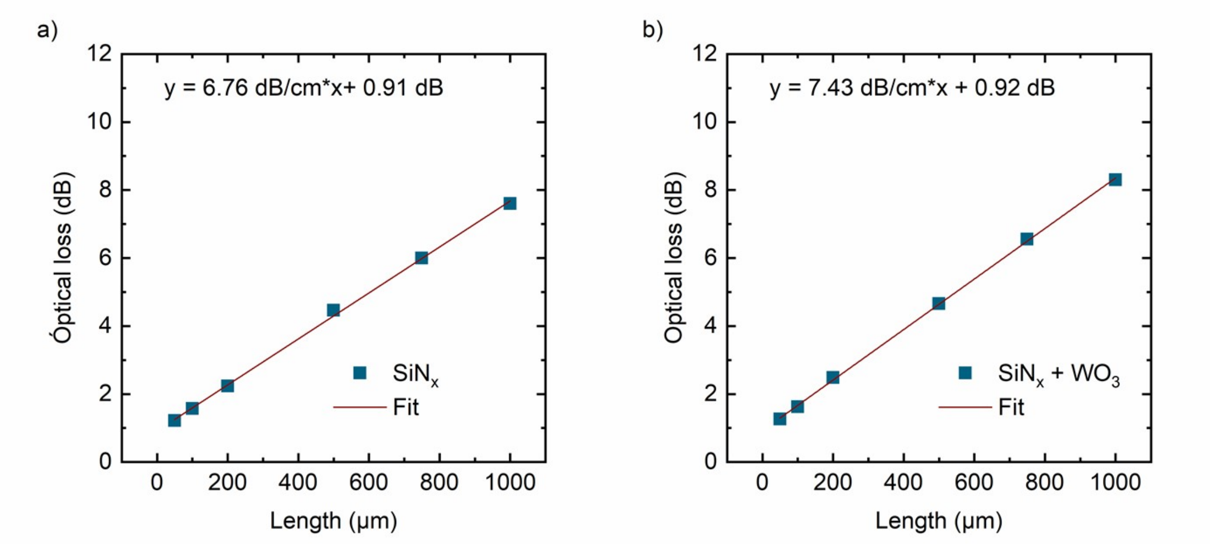

Fig. S3) Length-dependent waveguide optical loss at 1550 nm measured for a 2 µm wide and a 750 nm high SiN_x waveguide (a) without and (b) with a fully oxidized WO_3 modulation layer. y is the optical loss in dB and x is the waveguide length in µm.

Fig. S3 shows the waveguide optical loss at 1550 nm as a function of waveguide length. These measurements are performed to determine the loss per unit length for the SiN_x waveguide core, as well as the inherent loss induced by the fully oxidized WO_3 modulation layer. The linear fit indicates the optical loss for a SiN_x waveguide core having a 150 nm thick SiO_2 spacer and no WO_3 layer to be 6.8 dB/cm. The addition of WO_3 layer increases the optical loss by 0.64 dB/cm. In both waveguides, the y-intercepts of 0.91 dB and 0.92 dB are interpreted as coupling loss, which exceed the calculated coupling efficiency of 0.22. This discrepancy is attributed to the roughness of the end facets.

Tab. S1: Na^+ ion concentrations measured via an EC nanophotonic waveguide device and compared with the as-prepared values.

Prepared Na^+ Concentration (mM)	**Calculated Na^+ Concentration from ΔT (mM)**	**Error (%)**
25	26.9	-7.6
50	48.2	3.6
75	77.9	-3.9
100	87.9	12.1
150	141	6
200	195	2.5
250	257	-2.8
300	297	1
400	414	-3.5
500	491	1.8

Tab. S1 shows a comprehensive list of ion concentrations investigated with the introduced waveguide device. As can be seen from the table, the measured concentrations are within a 7.6% error window, with one major outlier. More averages per measurement or different calibration methods could potentially reduce this error further.

Tab. S2: Comparison of device performance for 100 mM $NaClO_4$ and $LiClO_4$ electrolytes

	Switching speed (90%)		**Max. modulation (CV)**	**Retention (2000 cycles)**
	Off	On		
Na^+	t = 0.56 s	t = 0.48 s	4×10^5	1.2×10^5
Li^+	t = 0.47 s	t = 0.51 s	5.3×10^5	6.7×10^4

Tab. S2 shows the comparison of device performance for 100 mM electrolytes containing either Na^+ or Li^+ ions. Switching speeds are measured as presented in Fig. S4, while the maximum achievable modulation and retention of modulation after 2000 cycles for Li^+ are compared to the experiment presented in Fig. 4.

Tab. S3: Device performance of several different optical waveguides utilizing EC WO_3

	Switching speed (90%)		Max. modulation	Platform
	Off	On		
Agrawal *et al.*[1]	2 s < t < 5 s	2 s < t < 5 s	0.04	Plasmonic/liquid electrolyte
Hopmann *et al.*[2]	t = 3.3 s	t = 8.42 s	$< 10^4$	Plasmonic/Solid state
Kim *et al.*[3]	t = 0.4 s for 30% modulation t = 10 s for 80% modulation		0.15	Photonic/liquid electrolyte
Kim *et al.*[4]	t = 3.2 s	t = 6.9 s	0.06	Photonic/liquid electrolyte
This work	t = 0.56 s	t = 0.48 s	10^6	Photonic/liquid electrolyte

Tab. S3 summarizes key device performance data for electrochromic waveguides reported to date. When compared to other devices of its class, the presented device exhibits exceptional transmission modulation and switching speed.

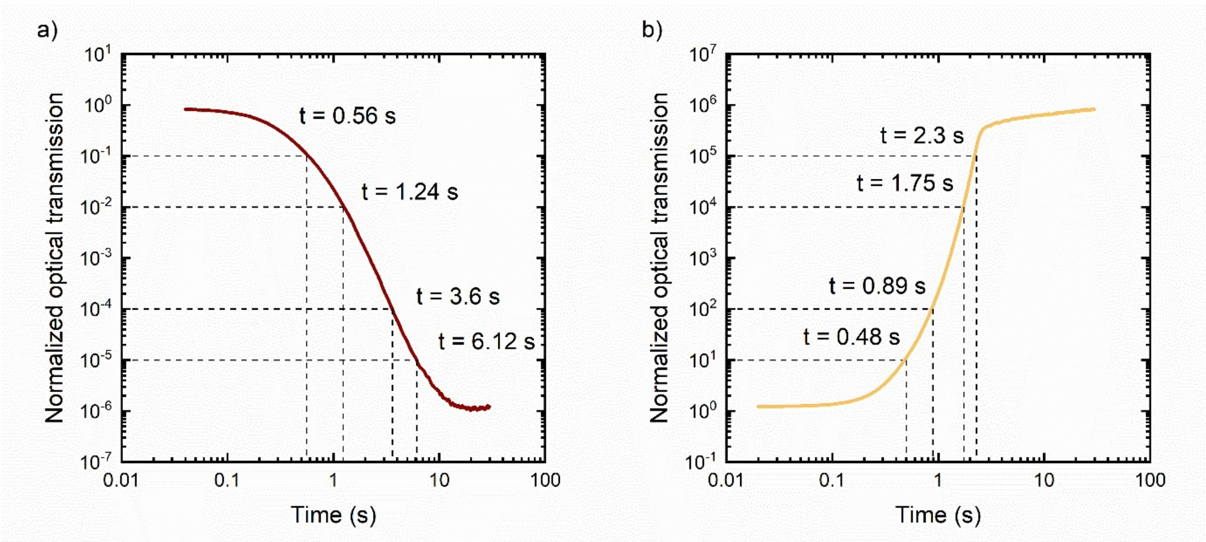

Fig. S4: Optical transmission as a function of time for: (a) intercalation of Na^+ ions at an applied voltage of 1.5 V and (b) deintercalation of Na^+ ions at an applied voltage of -1.5V. The indicated times correspond to the nearest dashed line's intercepts with the curves.

Fig. S4 depicts the optical transmission as a function of time for the intercalation and deintercalation process. For the intercalation (Fig. S4(a)), modulation of 10% and 1% are achieved at 0.56 s and 1.24 s respectively, and reaches 10^{-5} at 6.12 s. However, the recovery of the optical transmission is much faster, reaching 10^5 from the minimum value of 1 in only 2.3 s. This indicates that the deintercalation process is faster than the intercalation process.

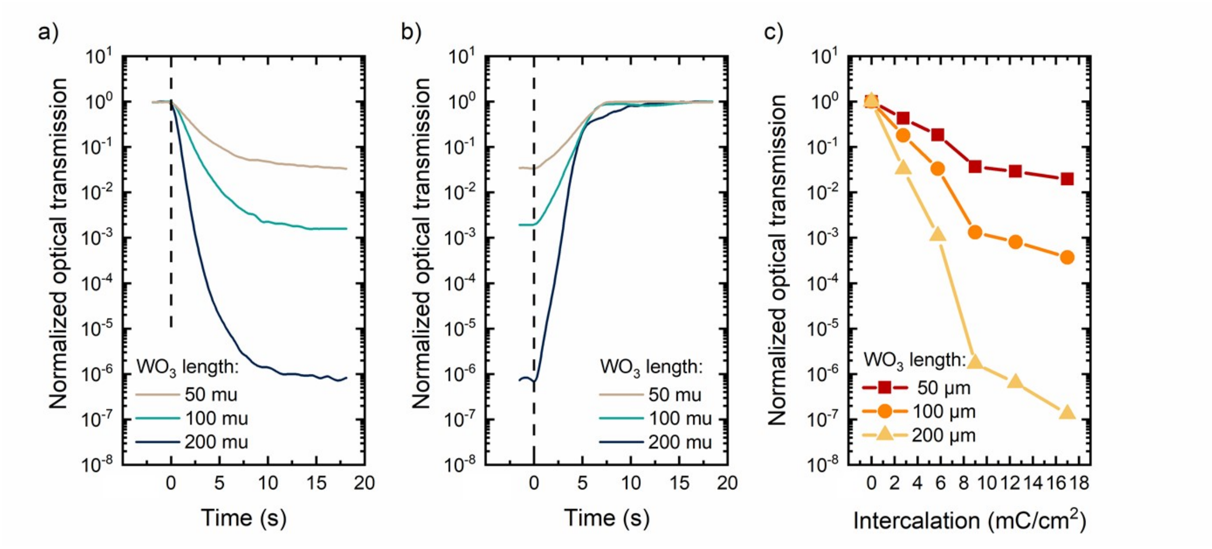

Fig. S5: Waveguide length dependent optical transmission as a function of time and Na^+ ion intercalation. (a) Optical transmission for 50 µm, 100 µm and 200 µm long EC nanophotonic waveguide over time when a voltage of + 1.5 V is applied. (b) Optical transmission for 50 µm, 100 µm and 200 µm long EC nanophotonic waveguide over time when a voltage of - 1.5 V is applied. (c) Simulated optical transmission for different intercalation levels for different EC nanophotonic waveguide lengths.

Fig. S5 shows the optical transmission time evolution for EC nanophotonic waveguides having different lengths during intercalation (a) and deintercalation (b). As seen in the figure, the length of the waveguide directly determines the available modulation depth. (c) Shows the intercalation dependent simulated transmission of waveguides with the same lengths as in (a,b). As can be seen, the maximum achievable transmission depth of the simulated devices is higher than that of the real devices. For a 200 µm waveguide length, the achieved modulation depth here is 10^6, while the simulated device shows a modulation depth of 10^7.

1. Agrawal, A., Susut, C., Stafford, G., Bertocci, U., McMorran, B., Lezec, H. J. & Talin, A. A. An integrated electrochromic nanoplasmonic optical switch. *Nano Lett.* **11**, 2774–2778 (2011).

2. Hopmann, E., Carnio, B. N., Firby, C. J., Shahriar, B. Y. & Elezzabi, A. Y. Nanoscale All-Solid-State Plasmochromic Waveguide Nonresonant Modulator. *Nano Lett.*

acs.nanolett.0c04315 (2021) doi:10.1021/acs.nanolett.0c04315.

3. Kim, J. T., Song, J. & Ah, C. S. Optically Readable Waveguide-Integrated Electrochromic Artificial Synaptic Device for Photonic Neuromorphic Systems. *ACS Appl. Electron. Mater.* (2020) doi:10.1021/acsaelm.0c00314.

4. Kim, J. T., Song, J., Ryu, H. & Ah, C. S. Electrochromic Infrared Light Modulation in Optical Waveguides. *Adv. Opt. Mater.* **8**, 1–8 (2020).